Numerical Simulation of Cell Venting within a Simplified 18650 Li-Ion Battery Pack

Daniel Grimmeisen[1], Marc S. Schneider[1]

[1]Cascate GmbH

1 Abstract

Violation of nominal operating conditions in Li-ion batteries can lead to internal damage and failure of the cells. This usually triggers chemical reactions that produce a large volume of hot gas. As a safety feature, 18650 battery cells are equipped with a safety vent. Once an internal pressure threshold is exceeded, the vent opens, and the gas escapes the cell at a high velocity to prevent uncontrolled structural failure. Within a battery pack, the hot gas needs to be guided to exit the pack while at the same time keeping neighbouring battery cells cool enough to stay within the safe temperature range. CFD simulation offers the capabilities to explore the mechanism of battery cell venting and flow guidance. This paper describes how such a simulation can be set up and run. Several steps are necessary to achieve this. First, Simcenter Battery Design Studio is used to model the 18650 battery cells. However, it is also described how this step can be avoided if certain prior knowledge about the process is available. Simcenter STAR-CCM+ is used for that and all subsequent steps. The cells are then assembled to a battery module and placed within a simplified battery pack housing.
Then, the module is discharged with a constant current while one battery cell is heated by a constant volumetric heat source. Once this cell reaches a pre-defined average temperature, it is assumed to fall in the regime of venting. Thus, in the next step hot gas is blown into the pack domain through the vent at a high velocity. The gas flows through the pack and escapes through an outlet on the opposing side, passing the neighbouring cells. During this process, the average temperatures of these cells are constantly monitored to evaluate the chance of thermal runaway propagation.

2 Introduction

With the rising importance of electric mobility, regulations to ensure occupant protection are developed at equal pace. Li-Ion batteries, while having a high volumetric and gravimetric energy density, are prone to failure if not controlled scrupulously by a battery management system. One possible failure mechanism is thermal runaway, during which the battery will continue to heat itself once a temperature threshold is surpassed. This can happen due to too fast charging or discharging, (dis)charging at too high temperatures, overcharging, or internal damage such as short circuits.

Although a characterisation of the thermal runaway proved to be difficult and highly dependent on factors such as cell chemistry, state of charge and temperature, the main steps of the thermal runaway process are well known (e.g. [1]):

1. the SEI layers (solid electrolyte interface) at the electrodes decompose, releasing energy
2. the intercalated lithium ions that sit in the electrodes start to react with the electrolyte between the electrodes in an exothermic reaction
3. the cathode starts to react with the electrolyte, releasing oxygen that is necessary for combustion processes
4. decomposition of the electrolyte

Since combustion processes happen in the cell during runaway, temperature and pressure rise fast once runaway occurs. To relieve pressure, a safety vent is installed in cylindrical cells. The burst disk is destroyed once the pressure in the cell is too high, releasing a large volume of high temperature combustion gas. Measures must be taken to prohibit neighbouring cells from heating up, possibly also suffering thermal runaway. This paper aims to assess the processes during heat up of a battery module, and thermal runaway of a cell within the module. It is shown how neighbouring cells are affected once one cell undergoes venting. This is done with the help of numerical simulation in different time scales.

© 2021 Copyright by DYNAmore GmbH

3 Properties of the battery cell

As a first step, a Li-Ion battery cell needs to be chosen. It is difficult to obtain comprehensive data on a battery cell while at the same time having enough literature available to assess thermal runaway behaviour of the same cell. Thus, a 18650 cell with a Nickel Cobalt Aluminium cathode is used. A Li-Ion battery cell with this cathode formulation usually has a high energy density and a cycle life of around 300 cycles [2].

The cathode mainly (0.908 weight fraction) consists of the active material. The other components are an Ethylene-Propylene Copolymer binder (0.042 weight fraction) and conductivity aids of Graphite and Carbon Black. The active material is $Li_x(Ni_{0.80}Co_{0.15}Al_{0.05})O_2$. From here on, it is referred to as NCA to enhance readability. Since not all information is available with all sources, battery cells from different manufacturers are assumed to be equal for this work.

On the anode side, Graphite is mainly used (0.930 weight fraction) with an additional CMC binder.

The size of the battery cell can be derived from the naming convention. A 18650 cell has a diameter of 18 mm, a length of 65 mm and is round (0). Aside from the outer dimensions of the battery cell, the size of the burst disk must be determined. The burst disk acts as predetermined breaking point once the pressure within the battery cell exceeds a bursting pressure. While no information on the specific burst disk of the used battery cell is publicly available, Mier has conducted research on burst disks for commonly used cell formations [3]. The statistical measurements of opening areas as given in [2] range from 6.111 mm² to 9.773 mm². A circular burst disk located on the centre of the cathode tab with an opening area of 8 mm² is chosen for this paper.

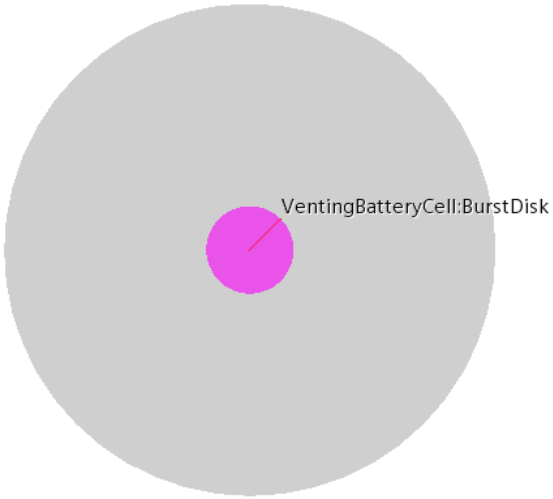

Fig.1: Location of the burst disk in the centre of the cathode tab of the venting battery cell

Fig.1 shows the location of the burst disk and the area compared to the area of the cathode tab of the battery cell, which has an area of 1018 mm².

To simulate the hot stream of gas that exits the battery cell through the burst disk, assumptions about the gas temperature and velocity must be made. For the given cell chemistry and conditions, [2] gives the temperature of the hot gas as 896 °C. An approach to calculate the exit velocity of the stream for numerical simulation is suggested by Kim [4]. For that, the mass loss of the battery cell over the venting as given in [2] is used. Divided by the duration of the venting, this yields the mass flow that leaves the battery cell. A mass loss of 20.5 g is given. A venting duration of 1 s - 10 s is given as well. Under the assumption of a venting duration of 5 s, this gives a mass flow of 4.1 g/s. Small-scale numerical tests showed that this mass flow equals to a velocity of 473 m/s at the burst disk. This velocity is used as an inlet velocity for the subsequent large-scale simulation.

© 2021 Copyright by DYNAmore GmbH

4 Physical domain

As a physical domain of the simulation, 7 battery cells are placed within a housing. Fig.2 shows a transparent view of the CAD model of the final setup.

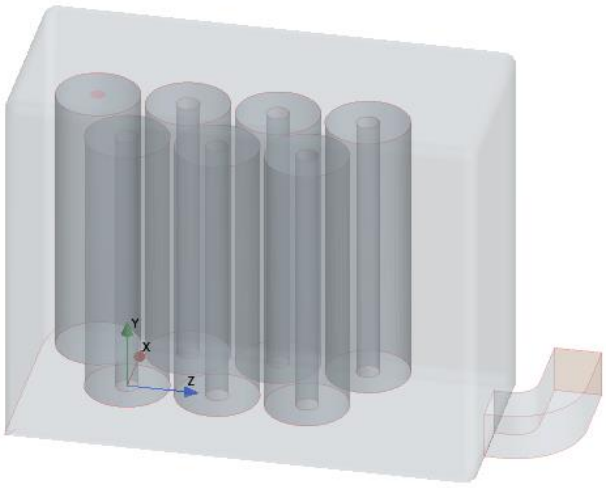

Fig.2: Virtual representation of the physical domain

The battery cells are arranged in a staggered grid to save space. The cells are separated by 3 mm to allow room for air circulation and thermal expansion although this is not part of the simulation. The housing is created so that enough air surrounds the cells in all directions. A channel allows for gas to be transported out of the domain. This is necessary to achieve mass conservation when the venting event happens. The left-most battery cell is specifically modelled to fail during the simulation. It hosts the venting event and the burst disk which will act as a gas inlet into the domain. This way, the hot gas passes the remaining 6 battery cells downstream towards the outlet. The housing is 100 mm x 80 mm x 44 mm, the channel outlet has an area of 10 mm x 10 mm. No connector parts nor mounting of the battery cells are part of this simulation.

5 Stages of the test

The simulation is divided into two stages: the first one leading to the venting event and the second one following the venting event. The first stage starts stationary with no flow within the surrounding housing nor electric or thermal load on the battery cells. The ambient temperature is 50 °C in all parts partaking in the simulation. Once the simulation starts a load of 20 A is prescribed on the circuit. This will lead to a sufficient heating of the battery cells. The volumetric heat that is generated in these cells per time step is monitored. One pre-determined battery cell is omitted from the electric load. To simulate its heating, the average volumetric heat of the other cells is used as a source term. This leads to the same temperature increase in all 7 cells. After 30 s, the pre-determined cell is declared to malfunction. To model this, the volumetric heat source term is increased by an arbitrary 10 % in this cell only. Subsequently, a higher temperature rise can be observed in this cell and its surroundings. In various experiments, Golubkov et al. found the onset temperature for thermal runaway to be between 136 °C and 140 °C for a state of charge between 75 % and 100 % [2]. Choosing one specific experiment, the onset temperature for thermal runaway is defined as 138 °C. The simulation is carried on until the malfunctioning battery cell reaches a maximum temperature of 138 °C. This completes the first stage.

The second stage of the simulation starts with the venting event. Assuming the battery management system would have shut off all electric discharge, the battery and circuit model are deactivated as well. The battery cells now act as hot bodies without internal heat source. They however still exchange heat with the surroundings. The second stage of the simulation observes the high temperature high velocity jet flow that exits through a burst disk in the malfunctioning battery cell. The hot gas distributes in the housing and the mixture leaves the domain through the outlet. This stage aims to determine how the other battery cells present in the module react to the hot gas flow that surrounds them and how their temperature increases. Ultimately, the simulation completes as soon as another battery cell reaches the threshold for thermal runaway at 138 °C.

© 2021 Copyright by DYNAmore GmbH

6 Numerical setup

Simcenter Battery Design Studio is used to model the NCA battery cell. Since this simulation covers the electro-thermal behaviour of the cell, the focus lies on the association between electrical and thermal behaviour of the cell. While technically, a physics-based battery model can be used to describe this coupling, it is more computationally efficient to use a substitution model that has been optimized to fit the expected load case. The RCR model is an equivalent circuit model that uses a schematic of resistors and capacitors to calculate the thermal response to an electrical load. In its smallest configuration the model uses only one resistor and no RC element (n = 0). To enhance accuracy, a higher number of RC elements can be used. In this paper, two RC elements are used (n = 2). A regression is performed to calibrate the RCR model towards the physics-based model within Simcenter Battery Design Studio.

In case Simcenter Battery Design Studio is not available to model the battery cell, another approach can be taken. If the heat that is generated by the battery cell as a response to an electrical load is known, this heat can be used as a source term on geometric battery parts that need to be created in CAD. This can only be achieved if experimental data on the thermal behaviour of the cell is known and if the load cycle and all its variations are known beforehand, since the heat generation depends on discharge current, state of charge and temperature.

Afterwards, the battery cell is imported into Simcenter STAR-CCM+. It must be noted that only the jellyroll of the cell is imported, omitting other parts like can, mandrel, and tabs. This is to facilitate simulation under the assumption that the other parts do not show a thermal response to an electrical load. The jellyroll is then multiplied and assembled into a 7-cell battery module, although only 6 cells are subjected to the thermal load.

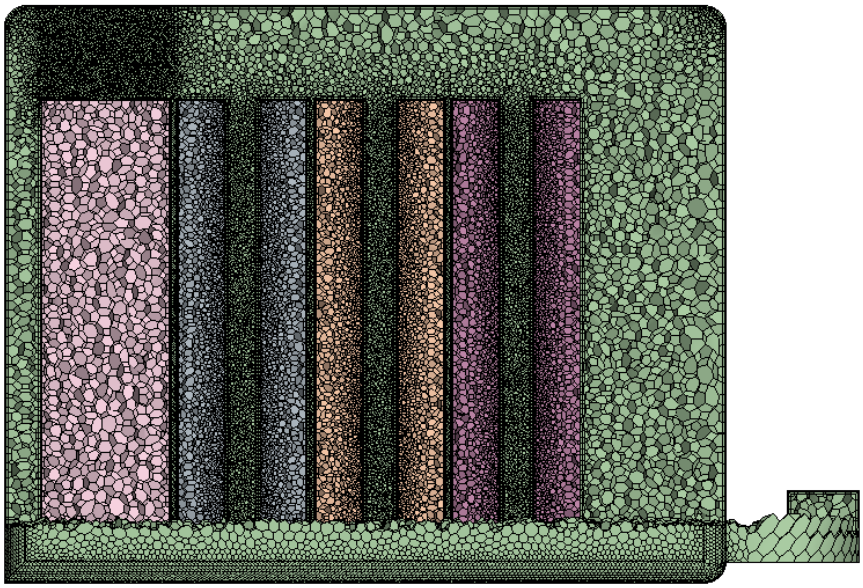

Fig.3: Polyhedral mesh and refinement for the gas jet near the burst disk

A computational mesh is generated for the housing and for the battery cells. The mesh is shown in Fig.3. Polyhedral cells are used for the volume mesh, prism layers are used in the near-wall boundaries of the fluid region. Approximately 150 000 cells are used to discretize the battery cells. Approximately 100 000 cells are used in the first simulation stage to model the housing. For the second stage, the domain is remeshed to account for the much higher velocity and temperature gradients in the housing. Around the jet flow, the mesh is refined even further. Altogether, the remeshed housing domain contains approximately 460 000 cells.

Velocity and temperature are given at the inlet where the hot gas jet exits the burst disk. The environmental pressure is given at the outlet where the expanded gas can leave the domain. The remaining outer wall boundaries of the housing allow convective heat transfer to an ambient temperature of 50 °C.

© 2021 Copyright by DYNAmore GmbH

To solve the transport equations a URANS solver is used. The conservation equations for mass and momentum are solved in a sequential manner. Turbulent closure is achieved using a K-omega model in the SST form. Since the time scales of the physical processes present in this simulation vary by magnitudes, different time step sizes were used for different stages of the simulation. Solving the energy equation usually requires a large time step because changes in temperature are small. This allows for a large time step in the energy dominated first stage of the simulation. With a time step of 0.5 s, the flow solution is quasi steady-state. After the venting event, the simulation is flow dominated with high velocities and accelerations. A time step of 1E-5 s is chosen for the time immediately after the venting event. Subsequently, once the flow has stabilized, the time step is increased to allow the slow changes of temperature within the battery cells to develop. The different time steps over the course of the simulation are shown in Table 1.

Table 1: Variation of time steps throughout simulation progress

Simulation stage	Until physical time	Time step	Number of steps
1	180.0000 s	5E-1 s	360
2	180.0020 s	1E-5 s	200
2	180.0200 s	1E-4	180
2	180.2930 s	1E-3	273

7 Results

Since the simulation was conducted in two stages, the results will be divided into two sections, one for each stage.

7.1 Heating of the battery module

Throughout the 180 s of the heating stage, the average battery state of charge fell from close to 100 % to 79.6 % under the load of 20 A. During the process, the 6 battery cells that were discharged behaved mainly uniformly. Fig.4 shows the temperature distribution over the battery cell surfaces. Note that the colour bar exaggerates the differences which don't exceed 0.2 °C after 1 minute of simulated time.

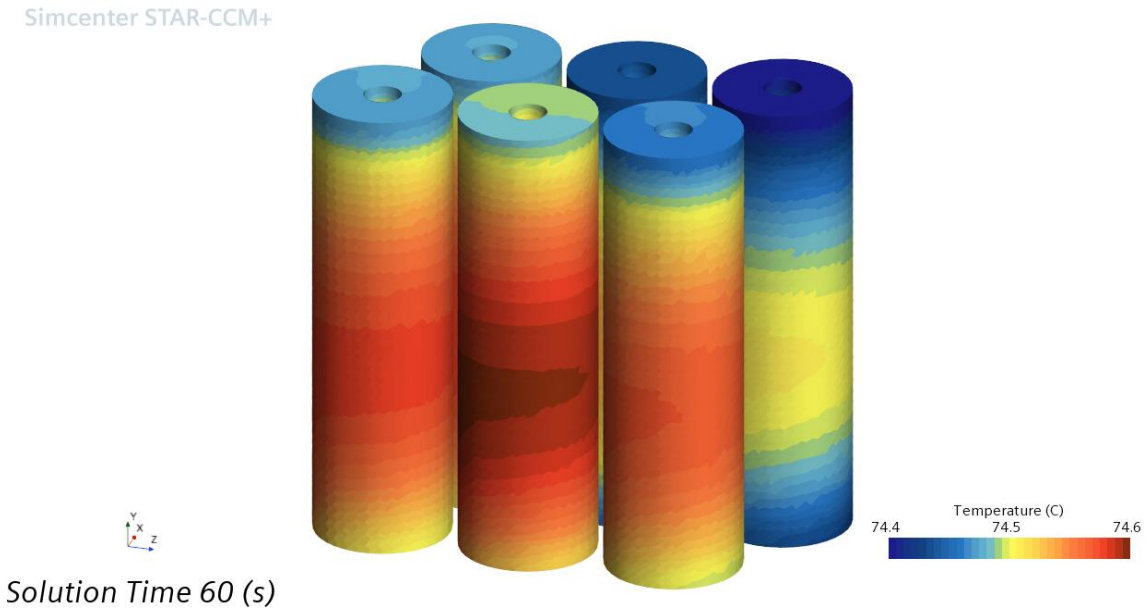

Fig.4: Uniformity of the temperature distribution on the battery cells (t = 60 s)

Fig.5 shows the temperature distribution within the jellyrolls were the jellyrolls unrolled. It is visible that the cells get hotter on one side compared to the other, even though the differences are small. The reason might be the way the cells are arranged. Cells with more air surrounding them see better cooling compared to cells near other cells. There is almost no temperature gradient from the inner layers towards the outer layers.

© 2021 Copyright by DYNAmore GmbH

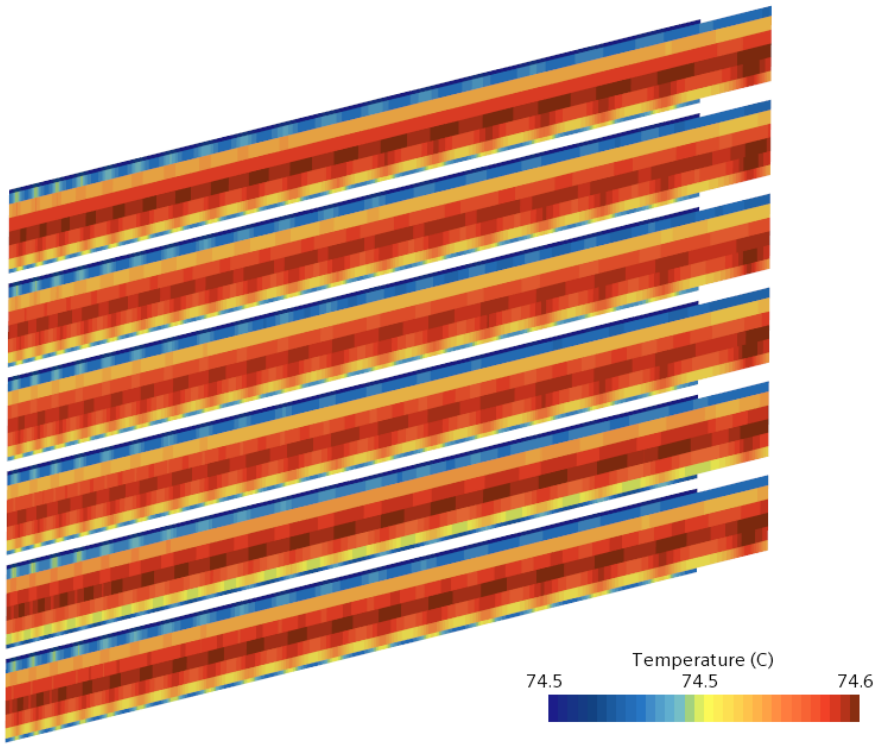

Fig.5: Unrolled view of the jellyrolls (t = 60 s)

Over the simulation, the volumetric heat generated within the battery cells appears to have an asymptotic limit. This is shown in Fig.6. After 30 s, the venting cell is considered to malfunction, and the volumetric heat has 10 % added.

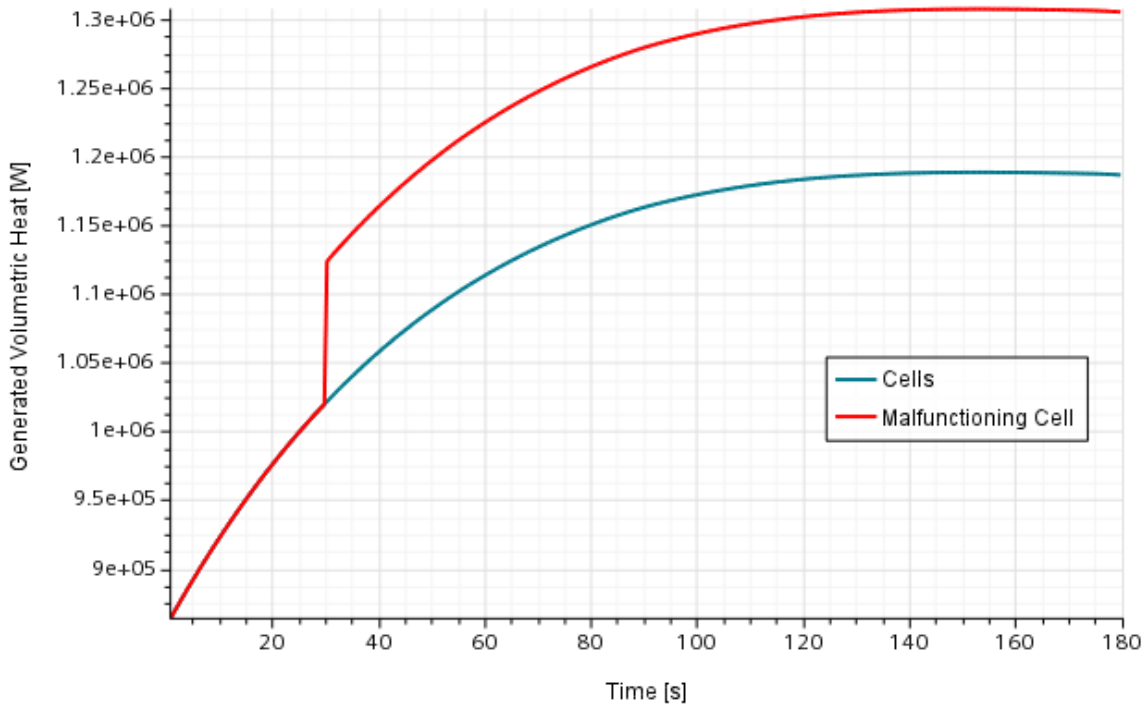

Fig.6: Generated volumetric heat with jump in malfunctioning cell after t = 30 s

© 2021 Copyright by DYNAmore GmbH

This can also be observed in the temperature diagram Fig.7. After 30 s, the temperature of the malfunctioning cell rises faster compared to its neighbours. However, a change of slope resulting from the jump in the heat generation diagram cannot be observed. This might be due to the higher temperature difference between battery cells and surroundings, transporting more heat into the surrounding air. The simulation stage is considered complete as soon as the temperature of the malfunctioning cell reaches 138 °C, the temperature for self-heating onset.

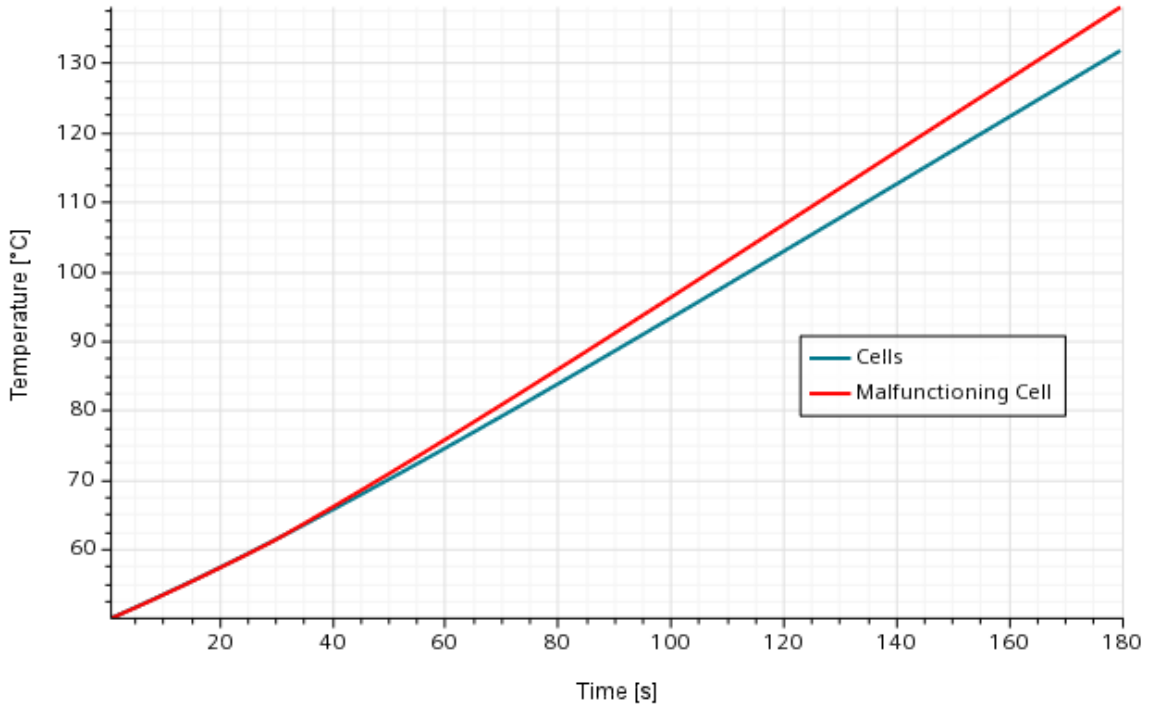

Fig.7: Temperature increase of the battery cells

7.2 Venting of the malfunctioning battery cell

Fig.8 shows the high temperature gas stream exiting the malfunctioning battery cell shortly after the venting event. The jet hits the wall, is deflected equally in all directions, and spreads through the domain.

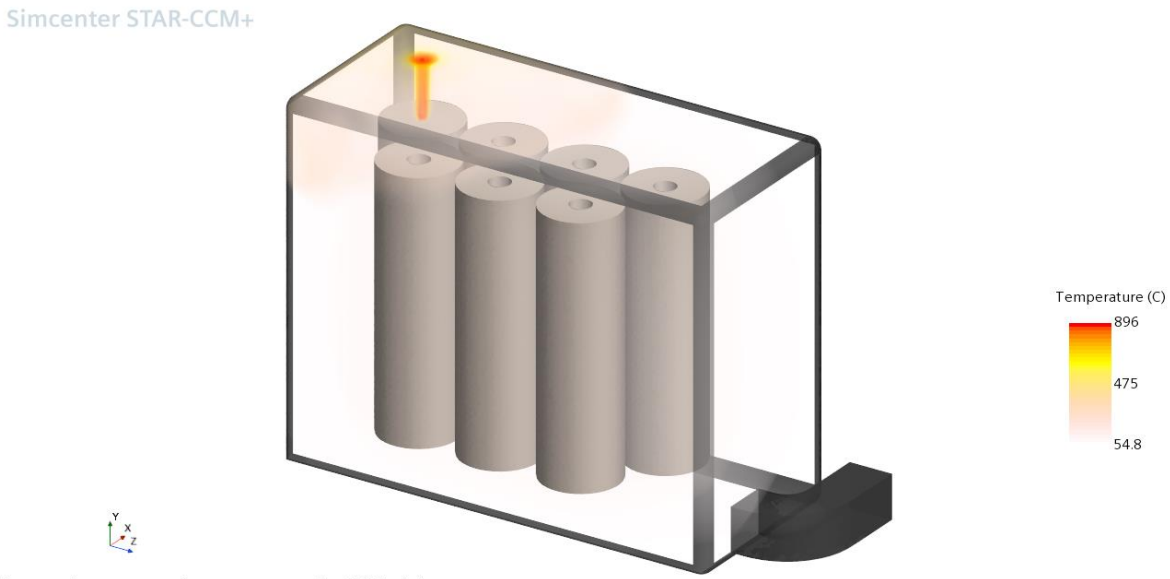

Fig.8: Hot gas stream exiting the burst disk of the malfunctioning battery cell (t = 180.001 s)

© 2021 Copyright by DYNAmore GmbH

A look at the streamlines in Fig.9 later during the simulation shows that the stream does not mainly sweep over the cells towards the outlet, but rather swirls close to the back side of the domain towards the bottom. The flow is highly turbulent and unsteady.

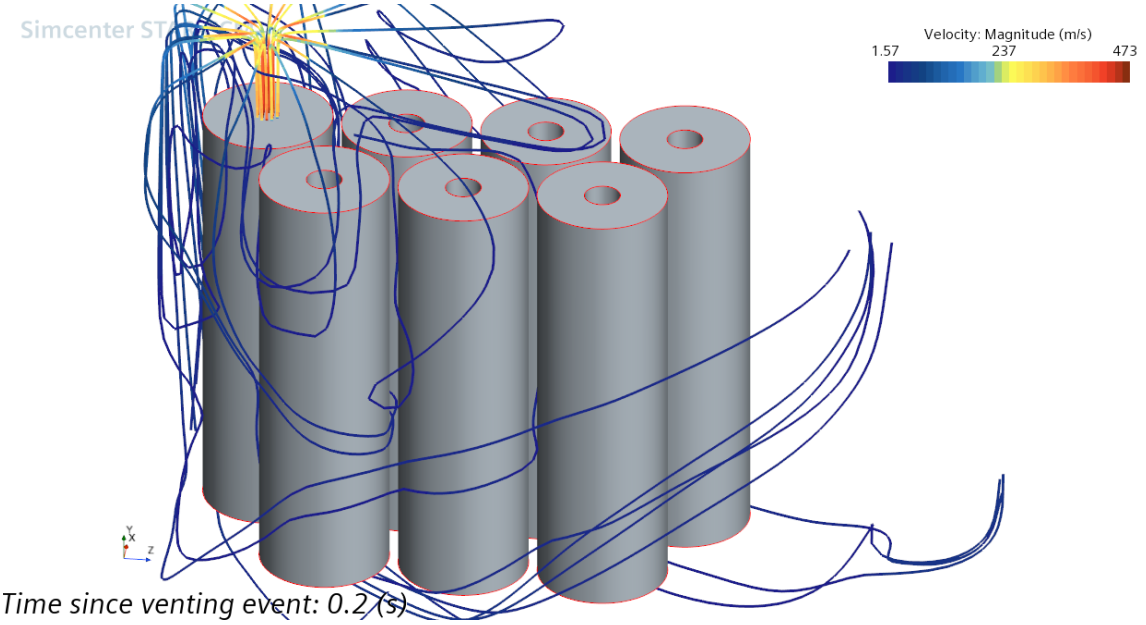

Fig.9: Streamlines of the gas exiting the cell through the burst disk (t = 180.2 s)

A plot of the temperature increase of the battery cells is shown in Fig.10. Almost immediately after the hot stream reaches the cell, the maximum temperature on its surface increases. The battery cells closer to the malfunctioning cell see the hot stream earlier than those further away.

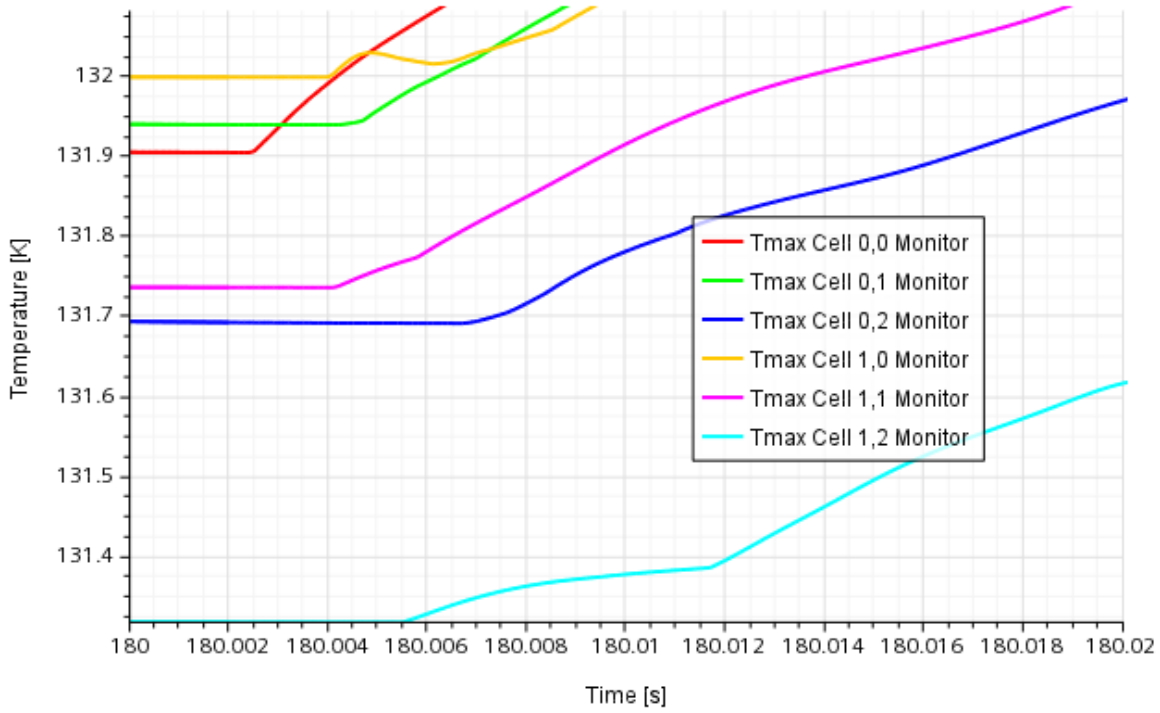

Fig.10: Temperature increase in the battery cells (t = 180 s to t = 180.02 s)

© 2021 Copyright by DYNAmore GmbH

Fig.11 shows the same plot on a larger scale. With the help of this plot, it can be calculated that it takes 0.275 s for the next battery cell to reach the point of thermal runaway at 138 °C. This would lead to a chain reaction in the module during which each cell would presumably suffer thermal runaway. The next battery cell to reach thermal runaway is the one closest to the malfunctioning cell, as it is subjected to the most heat.

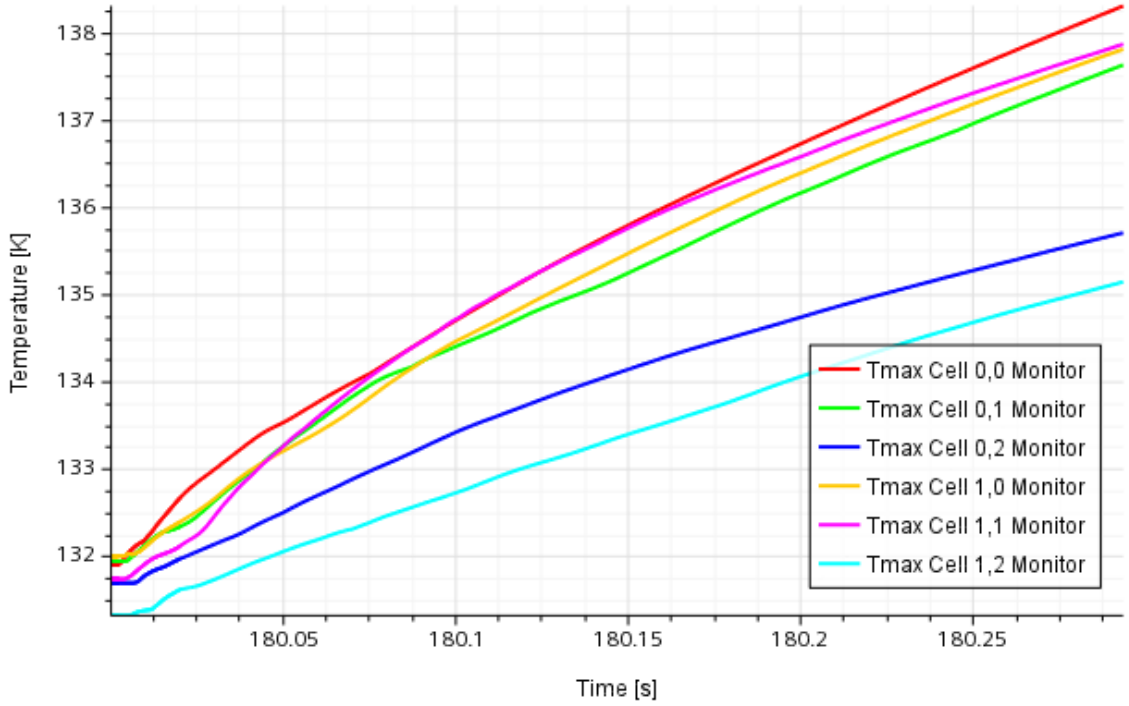

Fig.11: Temperature increase in the battery cells (t = 180 s to end)

8 Summary

In this paper it has been shown that it is feasible to simulate both the heating of battery cells within a module when prescribed an electrical load, as well as the safety venting of the hot combustion gases after one cell has reached the regime of thermal runaway. It has been determined that the main challenges when conducting such simulations are to obtain data on the battery cells and to make assumptions on the characteristics of the thermal runaway and venting processes.

For the test case at hand, it has been shown that while it takes 3 minutes for the first battery to reach self-heating temperature, it only takes 0.275 s for the next battery to reach this threshold temperature without cooling. Thus, it is vital to implement a form of cooling in the battery management system, although it must be shown that any cooling strategy is viable to transport the heat that is generated in the venting cell away.

For future consideration, there are assumptions that should be investigated further to setup a more credible simulation, some of which are:

1. Most assumptions regarding the hot gas flow (duration of venting, composition of venting gas and molar mass, additional reaction heat, time-dependent mass flow rate etc.)
2. Suitability of maximum temperatures in the cells as onset point for venting; battery cells might be resilient towards local overheating without reaching the regime of thermal runaway
3. Diameter and topological resolution of the burst disk
4. Protective parts for the jellyroll that might transport heat away before the high temperatures reach the jellyroll

© 2021 Copyright by DYNAmore GmbH

9 Literature

[1] Zhao, W. et al., „Experimental Analysis of Thermal Runaway in 18650 Cylindrical Li-Ion Cells Using an Accelerating Rate Calorimetry”, Batteries, 3, 2017

[2] Golubkov, A.: "Thermal runaway of commercial 18650 Li-ion batteries with LFP und NCA cathodes – impact of state of charge and overcharge", RSC Advances, 5, 2015, 57171-57186

[3] Mier, F. A.: “Measurement of 18650 format Lithium Ion battery vent mechanism flow parameters”, New Mexico Institute of Mining and Technology, 2018

[4] Kim, J.: “Modeling cell venting and gas-phase reactions in 18650 lithium ion batteries during thermal runaway”, Journal of Power Sources, March 2021

© 2021 Copyright by DYNAmore GmbH